

# Projection Valued Measure-based Quantum Machine Learning for Multi-Class Classification

Won Joon Yun, Hankyul Baek, and Joongheon Kim, *Senior Member, IEEE*

**Abstract**—In recent years, quantum machine learning (QML) has been actively used for various tasks, e.g., classification, reinforcement learning, and adversarial learning. However, these QML studies do not achieve complex tasks due to scalability issues on input and output are the biggest hurdle in QML. To cope with this problem, we aim to solve the output scalability issue. Motivated by this challenge, we focus on *projection-valued measure (PVM)* which utilizes the nature of probability amplitude in quantum statistical mechanics. By leveraging PVM, the output dimension is expanded from the number of qubits  $q$  to  $\mathcal{O}(2^q)$ . We propose a novel QML framework for multi-class classification. We corroborate that our framework outperforms the *state-of-the-art (SOTA)* with various datasets using no more than 6 qubits. Furthermore, our PVM-based QML outperforms 42.2% SOTA.

**Index Terms**—Quantum Computing, Quantum Convolutional Neural Network, Quantum Machine Learning.

## I. INTRODUCTION

IBM Quantum has publicized the 2022 development roadmap that 10–100k qubits quantum computers will be developed until 2026 [1]. Spurred by the recent advance of quantum computers, many theoretical quantum supremacies are corroborated [2]. Nowadays, quantum computing is a strong candidate to replace classical computing in the near future. These trends have derived many research areas in the form of combining existing fields with quantum computing. Quantum machine learning (QML) is one of the emerging topics in quantum computing [3]–[5]. The initiation of QML has started re-implementing the existing machine learning (ML) solutions and neural networks (NN) using quantum neural networks (QNN) [6], [7], e.g., image classification [8], [9], reinforcement learning [10], [11], and federated learning (FL) [12]. Because QML has been attracted recently, it is still an infant compared to ML [13]. In addition, it also has important challenges to resolve, e.g., scalability, trainability, and difficulty in simulating on a large scale [14]. For an innovative solution, quantum convolution neural network (QCNN) has resolved trainability [15] and scalability on input data [8].

However, QML is still suffered from scalability on outputs. Thus, QML has been studied regarding simple tasks (e.g., binary classification [16]–[20]), or deploy classical NN at the end of QNN (i.e., quantum-classical hybrid computing [21]–[23]). Despite the importance of pure QML to have insights into quantum supremacy, the multi-class classification with a pure quantum version has not been considered yet.

This research was funded by the National Research Foundation of Korea (2022R1A2C2004869). (Corresponding author: Joongheon Kim).

Won Joon Yun, Hankyul Baek and Joongheon Kim are with the School of Electrical Engineering, Korea University, Seoul 02841, Republic of Korea (e-mails: {ywjoon95, h7back, joongheon}@korea.ac.kr).

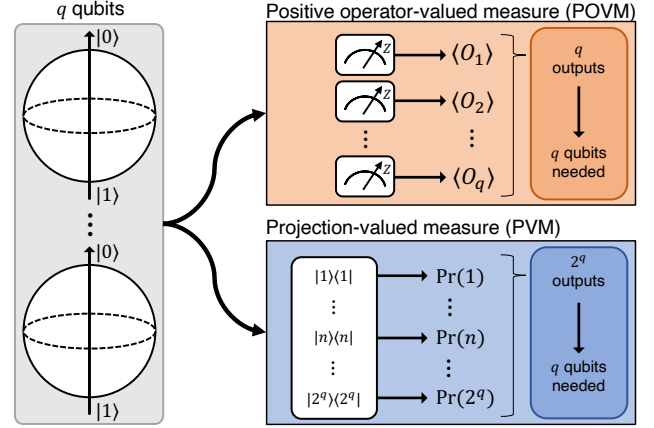


Fig. 1. The difference between POVM and PVM. In this paper, we utilize POVM for image processing as well as PVM method for multi-class prediction.

Motivated by these trends, we propose the methodology for how QML successfully achieves multi-class classification. First of all, we investigate quantum measurement theory and its applications. Most quantum computers and QML frameworks follow the *positive operator-valued measure (POVM)* to obtain the output [24]. However, the size of the POVM-based output in  $q$ -qubit system cannot exceed the number of qubits, i.e.,  $\mathcal{O}(q)$  and this hinders the output of QNN scalable. We focus on the *projection-valued measure (PVM)*, which is a special form of POVM [25]. By utilizing PVM in QNN, we can make  $\mathcal{O}(2^q)$  outputs (named observables) by utilizing whole bases of  $q$ -qubits. By using this nature of PVM, we propose the *quantum machine learning framework for multi-class classification* without using any classical NN methodologies. In addition, we propose a probability amplitude regularizer which makes observables fit the true label. This significantly improves the performance of QML framework.

**Contributions.** The contributions of our proposed QML framework are listed as follows.

- We first propose a novel PVM-based QNN for multi-class classification. In addition, we do not use any classical NN methodologies. Our proposed QML framework provides an insightful bridge between quantum computing research and machine learning research.
- Moreover, we show the quantum supremacy in QCNN computation operations by comparing the computational complexity to classical NN methodologies.
- Finally, we improve the scalability of QML without classical NN methodologies regarding input with up to  $32 \times 32 \times 3$  and output up to 26 classes, respectively.

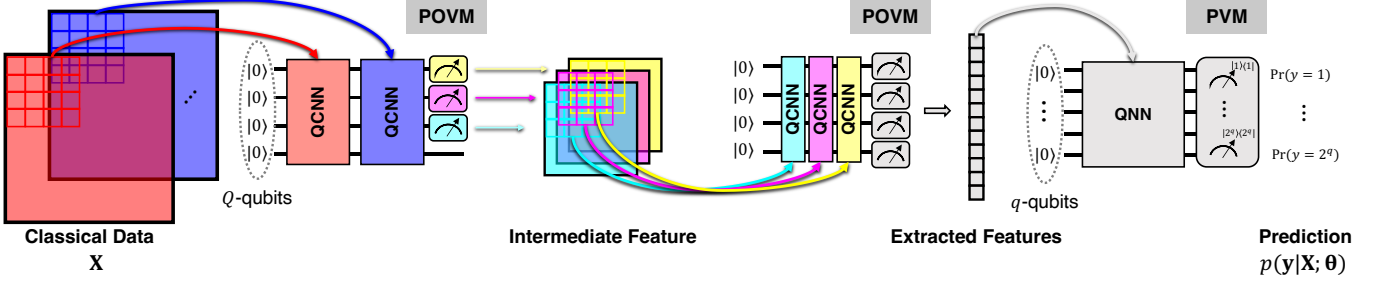


Fig. 2. The computing processes on QCNN and QNN. Each color (e.g., red, blue, yellow, magenta, or cyan) indicate the channel. Each 2D grid indicates the patch in each channel. When the quantum state is measured in QCNN, the expected value of projection for each qubit stands as the value of the output channel. The extracted features are vectorized classical data, which is given as an input of QNN. QNN makes a probability measure that corresponds to the prediction of classes.

## II. PRELIMINARIES: QUANTUM MACHINE LEARNING

### A. Notation and Mathematical Setup

In this paper, we use notations  $\Theta = \{\theta^{\text{enc}}; \theta^{\text{PQC}}\}$  for trainable parameters. We define  $\zeta \triangleq \{(\mathbf{X}, \mathbf{y})\}$  as a sampled mini-batch where  $\mathbf{X}$  and  $\mathbf{y}$  stand for the sampled input data and the corresponding labels from mini-batch, respectively. The labels  $\mathbf{y} \triangleq \{y_n\}_{n=1}^{|\mathbf{y}|}$  are one-hot vectors where  $y_n = 1$  if the true labels are  $n \in \mathbb{N}[1, |\mathbf{y}|]$ , and the other elements are 0. The extracted features are denoted as  $\hat{\mathbf{X}}$ . To represent the quantum state and its operations, Dirac-notation is used. In addition, the operators  $(\cdot)^\dagger$  and  $\otimes$  stand for complex conjugate transpose and tensor product, respectively. We use the two terms  $Q$  and  $q$  separately to indicate a  $Q$ -qubit system that encodes classical data and a  $q$ -qubit system that performs prediction. The  $Q$  qubit quantum state is defined as follows,

$$|\psi\rangle = \sum_{n=1}^{2^Q} \alpha_n |n\rangle, \quad (1)$$

where  $\alpha_n$  and  $|n\rangle$  stand for the probability amplitude and  $n$ -th basis in Hilbert space, respectively. By the definition of Hilbert space (i.e.,  $\mathcal{H}^{\otimes Q} \equiv \mathbb{C}^{2^Q}$ ), probability amplitude  $\forall \alpha_n \in \mathbb{C}$  has following relationship, i.e.,  $\sum_{n=1}^{2^Q} |\alpha_n|^2 = 1$ .

### B. Quantum Measurement Theory for Classification

In measurement theory, two main streams exist in the literature, i.e., POVM and PVM [25]. In POVM, it generates outputs as follows. The quantum state is projected into Pauli-Z measure devices for every qubit, where Pauli-Z is  $\mathbf{Z} = \text{diag}(1, -1)$ . The  $n$ -th projection matrix is defined as  $\mathbf{P}_n \triangleq \mathbf{I}^{\otimes n-1} \otimes \mathbf{Z} \otimes \mathbf{I}^{\otimes Q-n}$ , where  $\mathbf{I}$  stands for  $2 \times 2$  identity matrix, respectively. In POVM, it makes the expectation value of a projection  $\mathbf{P}_n$  as random variable denoted as  $O_n \in \mathbb{R}[-1, 1]$  where  $\forall n \in \mathbb{N}[1, Q]$ . Its expectation value of  $m$ -th qubit is  $\langle O_n \rangle = \langle \psi | \mathbf{P}_n | \psi \rangle$ . According to [25], the expectation value of a projection can be used with the softmax function and temperature parameter  $\beta \in \mathbb{R}$  to make a prediction for  $q$ -classes as follows,

$$\Pr_{\text{POVM}}(y = n) = \frac{\exp(\beta \langle O_n \rangle)}{\sum_{n=1}^q \exp(\beta \langle O_n \rangle)}. \quad (2)$$

Note that the number of qubits  $q$  should satisfy  $q \geq |\mathbf{y}|$  in POVM. In addition, POVM with classical NNs is widely used to make large-scale predictions without the condition  $q \geq |\mathbf{y}|$ . In this paper, we consider PVM for classification where it is a special type of POVM. The PVM makes a probability measure by projecting the quantum state into projector  $\{|n\rangle\langle n|\}_{n=1}^{2^q}$ , and the output can be expressed as follows,

$$\Pr_{\text{PVM}}(y = n) = \langle \psi | n \rangle \langle n | \psi \rangle = |\langle \psi | n \rangle|^2 = |\alpha_n|^2. \quad (3)$$

Note that the output of PVM is probability distribution where  $\Pr_{\text{PVM}}(y = n) = \sum_{n=1}^{2^q} |\alpha_n|^2 = 1$ . In this paper, we use both POVM and PVM for image processing with QCNN as well as classification with QNN, respectively.

## III. QUANTUM MACHINE LEARNING FRAMEWORK FOR MULTI-CLASS CLASSIFICATION

### A. Architecture

Our QML framework for multi-class classification consists of QCNNs and QNN. The structure of a QCNN/QNN is tripartite: the state encoding, linear transform with parametrized quantum circuits (PQCs), and the measurement [26]. First of all, the classical input size is larger than the number of qubits, we consider data-reuploading [27] for state encoder. To successfully encode the classical input data  $\mathbf{X}$ , the  $\mathbf{X}$  is splitted into  $[\mathbf{x}_1; \dots; \mathbf{x}_{c_{\text{in}}}]$ . The classical splitted data are encoded to probability amplitude, where the encoding process can be expressed as follows,

$$|\psi_{\text{enc}}\rangle = U(\theta_{c_{\text{in}}})U(\mathbf{x}_{c_{\text{in}}}) \cdots U(\theta_1)U(\mathbf{x}_1)|\psi_0\rangle, \quad (4)$$

where  $|\psi_0\rangle$  denotes the initial quantum state, e.g., the first standard basis of  $2^Q$ -dimensional vector and  $\forall \theta_c \in \theta_{\text{enc}}$ , and  $\forall c \in \mathbb{N}[1, c_{\text{in}}]$ . The encoded state  $|\psi_{\text{enc}}\rangle$  is processed with PQCs where the result is presented as  $|\psi_{\text{PQC}}\rangle = U(\theta^{\text{PQC}})|\psi_{\text{enc}}\rangle$ . The processed quantum state  $|\psi_{\text{PQC}}\rangle$  is measured by POVM in QCNN, and PVM in QNN, respectively.

### B. Pipeline

**POVM-based QCNN for Image Processing.** As presented in Fig. 2, QCNN takes input from classical data and returns the feature. Algorithm 1 (lines 2–13) presents the image processing with QCNN. In QCNN processing, the input has  $W \times H \times c_{\text{in}}$

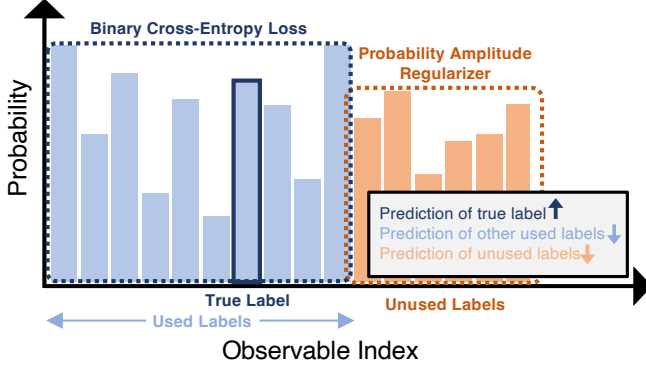


Fig. 3. The illustration of the objective function ( $|y| = 10$  and  $q = 4$ ). Two loss functions are used in this paper (i.e., binary cross-entropy loss and probability amplitude regularizer). Leveraging our proposed loss function, the prediction of true label is increased, the prediction of other used labels is decreased, and the prediction of unused labels is decreased, respectively.

shape. Note that  $\hat{W}$  and  $\hat{H}$  depend on the kernel size  $\kappa$ , stride  $s$ , and padding  $d$ , i.e.,  $\hat{W} = (W + d)/s$  and  $\hat{H} = (H + d)/s$ . Each patch of input is feed-forwarded to QCNN by data-reuploading method (4). The pooling of QCNN occurs by POVM. The  $n$ -th expected value of POVM  $\langle O_n \rangle$  corresponds to a scalar value of  $n$ -th channel. The output has  $\hat{W} \times \hat{H} \times c_{out}$  shape. The computational complexity of our QNN per layer is  $\mathcal{O}(\hat{W} \cdot \hat{H} \cdot \kappa^2 \cdot c_{in})$ , where  $\kappa$  denotes the kernel size, whereas the computational complexity of classical CNN is  $\mathcal{O}(\hat{W} \cdot \hat{H} \cdot \kappa^2 \cdot c_{in} \cdot c_{out})$ . Note that the input and output channels in QCNN are scalable under the constraint  $\forall c_{in}, c_{out} \in \mathbb{N}[1, Q]$ .

**PVM-based QNN for Classification.** In general, the number of classes  $|y|$  is larger than the number of qubits  $q$ . However, it is hard to train QCNN/QNN when the number of qubits is increased. Thus, softmax-based POVM such as (2) is limited to simple multi-class classification (e.g., binary classification or 4 classes classification). Thus, we consider the PVM-based QNN for classification, where the process is presented in Algorithm 1 (lines 14–20). Similiar to QCNN processing, the extracted features are encoded with (4). To enable multi-class classification, we design the measurement of QNN with PVM. Then, we can obtain the probability of  $2^q$  observables when a quantum state  $|\psi\rangle$  is projected into pure density matrices, i.e.,  $\{|1\rangle\langle 1|, \dots, |n\rangle\langle n|, \dots, |2^q\rangle\langle 2^q|\}$ . The probability of  $n$ -th class can be expressed as follows,

$$p_n = \Pr(y = n | \mathbf{X}; \Theta) = |\alpha_n|^2. \quad (5)$$

Note that our framework does not require softmax function to make logits to predictions. The probability amplitude  $\alpha_n$  is mapped to the probability of class  $n$  directly. In addition, our framework does not require softmax temperature coefficient [28]. However, our framework has error on probability due to the probability of unused classes.

### C. Training Algorithm

In this paper, we design a new regularizer to reduce training error because the probability of unused classes incurs the performance degradation. In Fig. 3, we compose the objective

Algorithm 1: QML Framework for Multi-Class Classification

```

1 Notation. Processing data  $\tilde{\mathbf{X}}$ , Processed data  $\tilde{\mathbf{X}}$ , stride  $s$ ,
   kernel size  $\kappa$ , and the number of QNN depths  $D$ ;
2 Image Processing( $\mathbf{X}$ ):
3    $\tilde{\mathbf{X}} \leftarrow \mathbf{X}$ ;
4   for  $w \in \{0, s, 2s, \dots, W - s\}$  do
5     for  $h \in \{0, s, 2s, \dots, H - s\}$  do
6       Initialize quantum state,  $|\psi\rangle \leftarrow |0\rangle$ ;
7       for  $c \in \{1, 2, \dots, c_{in}\}$  do
8         Prepare data,  $\tilde{\mathbf{x}} \leftarrow \tilde{\mathbf{X}}_{w:w+\kappa, h:h+\kappa, c}$ ;
9         Upload data,  $|\psi\rangle \leftarrow U(\theta_c) \cdot U(\tilde{\mathbf{x}}) \cdot |\psi\rangle$ ;
10      for  $c \in \{1, 2, \dots, c_{out}\}$  do
11        Measure through POVM and collects
          outputs,  $\tilde{\mathbf{x}}_{\frac{w}{s}, \frac{h}{s}, c} \leftarrow \langle O_c \rangle_{\tilde{\mathbf{x}}, \Theta}$ ;
12  Get intermediate feature,  $\tilde{\mathbf{X}} \leftarrow \tilde{\mathbf{X}}$ ;
13  Output: Extracted feature  $\tilde{\mathbf{X}}$ ;
14 Prediction( $\tilde{\mathbf{X}}$ ):
15  Initialize  $\mathbf{p} \leftarrow \emptyset$ ;
16  Prepare the pure density matrices,
     $\{|1\rangle\langle 1|, \dots, |n\rangle\langle n|, \dots, |2^q\rangle\langle 2^q|\}$ ;
17  for  $m \in \{1, \dots, 2^q\}$  do
18    Obtain prediction value of class  $c$ ;
19     $\mathbf{p} \leftarrow \mathbf{p} \cup p_c$ ;
20  Output: Prediction  $\mathbf{p}$ ;

```

function with binary cross-entropy function  $\mathcal{L}_{BCE}$  and *probability amplitude regularizer*  $\mathcal{L}_{PAR}$  for probability regarding unused class indices, which can be expressed as follows,

$$\mathcal{L}_{BCE}(\Theta; \mathbf{X}) = - \sum_{n=1}^{|y|} [y_n \log p_n + (1 - y_n) \log(1 - p_n)], \quad (6)$$

$$\mathcal{L}_{PAR}(\Theta; \mathbf{X}) = - \sum_{n' > |y|}^{2^q} \log(1 - p_{n'}), \quad (7)$$

where  $q \geq \lceil \log_2(|y|) \rceil$ . Thus, we finalize the train loss function for one-step single update as follows,

$$\mathcal{L}(\Theta; \zeta) = \frac{1}{|\zeta|} \sum_{(\mathbf{X}, \mathbf{y}) \in \zeta} [\mathcal{L}_{BCE}(\Theta; \mathbf{X}) + \mathcal{L}_{PAR}(\Theta; \mathbf{X})]. \quad (8)$$

Next, the gradient of train loss function can be obtained as follows. Because a quantum computer cannot use classical training methods, e.g., back-propagation with chain rule, the 0-th order optimization is utilized to estimate the gradient, called *parameter-shift rule* [29], [30]. By calculating the symmetric difference quotient of loss  $\mathcal{L}$ , the loss gradient is obtained as follows,

$$\frac{\partial \mathcal{L}(\Theta)}{\partial \theta_m} = \mathcal{L}\left(\Theta + \frac{\pi}{2} \mathbf{e}_m\right) - \mathcal{L}\left(\Theta - \frac{\pi}{2} \mathbf{e}_m\right), \quad (9)$$

where  $\mathbf{e}_m$  is one-hot vector that eliminate all components except  $\theta_m$ , i.e.,  $\Theta \cdot \mathbf{e}_m = \theta_m$  and  $\forall m \in \mathbb{N}[1, |\Theta|]$ . Finally, the trainable parameters in our QML framework are updated as  $\Theta \leftarrow \Theta - \eta \nabla_{\Theta} \mathcal{L}(\Theta)$ , where  $\eta$  is a learning rate.

## IV. PERFORMANCE EVALUATION

### A. Experiment Setup

In this section, we mainly investigate the trainability of our QML framework with various datasets and the impact of a

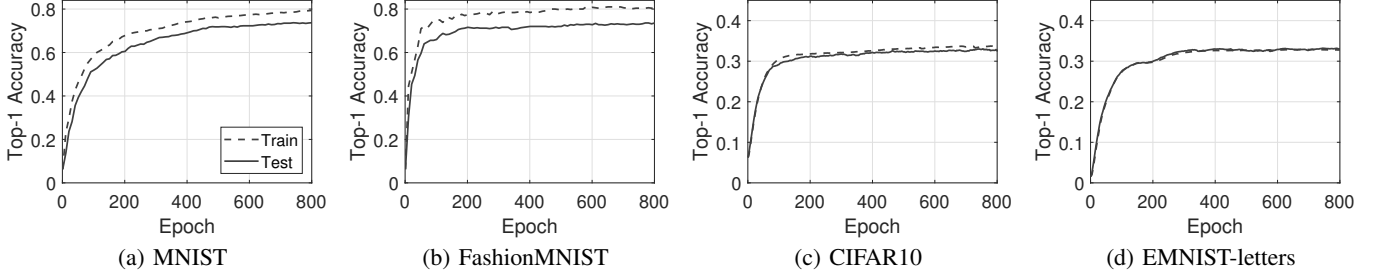
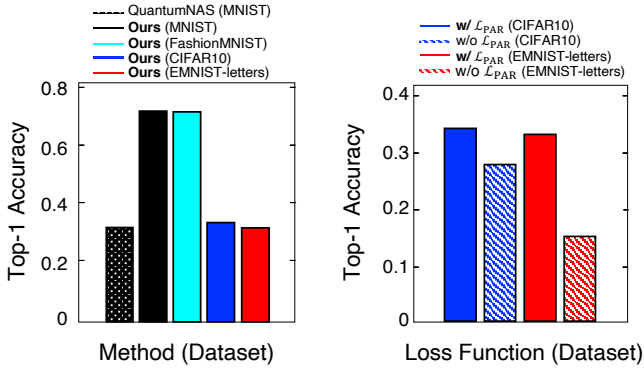


Fig. 4. Learning curve with various datasets.

TABLE I  
EXPERIMENTAL SETTINGS

Dataset	Input size	# of classes	# of qubits ( $q$ )
MNIST	$28 \times 28 \times 1$	10	4
FashionMNIST	$28 \times 28 \times 1$	10	4
CIFAR10	$32 \times 32 \times 3$	10	4
EMNIST-letters	$28 \times 28 \times 1$	26	6



(a) Comparison with SOTA [32] (b) Impact of Regularizer

Fig. 5. Additional experiments: (a) shows the comparison between our framework and QuantumNAS [32], and (b) shows the ablation study of probability amplitude regularizer.

probability amplitude regularizer via performance evaluation. For this, we benchmark the train accuracy, test accuracy, comparison to *state-of-the-art* (SOTA), and the ablation of regularizer. Because our main scope is to investigate the scalability of QML, we do not interpolate the input data size nor use selected classes. The datasets used in this paper are listed in Table I. We use two QCNN models for image processing where  $4 \times 4$  kernel is commonly used with stride  $s = 3$  where the kernels have 3 channels. Our framework utilizes 4 qubits and controlled unitary gates for all quantum circuits, *e.g.*, QCNN and QNN [31]. The hyperparameters used in this paper are as follows, *i.e.*, Adam optimizer,  $8 \times 10^{-3}$  for initial learning rate, and 1,024 for batch size. Note that all experiments for the proposed QML framework are conducted in classical computers with Python v3.8.10 and torchquantum [32].

### B. Numerical Results

**Trainability.** Fig. 4 shows the learning curves with various datasets. Our framework converges to sub-optimal for all

datasets. In Fig. 4(a), the test accuracy increases from 6.25% to 74.2%, and the domain gap between the trainset and the testset presents as 5.7% between the top-1 accuracies. In Fig. 4(b), the test accuracy grows from 6.25% to 73.8%, where 6.8% gap exists. In Fig. 4(c)/(d), the top-1 accuracies for CIFAR10 and EMNIST-letters show 34.4% and 33.1%, respectively, and the domain-gap between trainset and testset is lower than MNIST and FashionMNIST.

**Comparison to SOTA.** We compare our framework to QuantumNAS [32]. According to [32], the input is  $6 \times 6$  sized MNIST images, and QuantumNAS considers deploying on the quantum devices where quantum noise exist. However, we benchmark our framework with the original size of the dataset as shown in Table I without considering quantum noise. As shown in Fig. 5(a), our framework outperforms QuantumNAS 44.2% regarding top-1 accuracy given MNIST dataset. Moreover, our framework is benchmarked with various datasets, *i.e.*, FashionMNIST, CIFAR10, EMNIST-letters using less than 7 qubits, whereas QuantumNAS uses 10 qubits. In summary, PVM enables not only multi-class classification but also achieves higher accuracy than SOTA.

**Ablation Study of Regularizer.** In this paper, we propose a *probability amplitude regularizer*. We conduct an ablation study of the regularizer with two datasets (*i.e.*, CIFAR10, EMNIST-letters). As shown in Fig. 5(b), the top-1 accuracy of the training scheme with  $\mathcal{L}_{PAR}$  outperforms 7.5% for CIFAR10 and 17.8% for EMNIST-letters. It is because the prediction of other used labels is decreased via the probability amplitude regularizer. Thus, our proposed regularizer is significant in our QML framework for multi-class classification.

## V. CONCLUSIONS AND FUTURE WORK

We aim to expand the limited input and output dimension of QML and to compute multi-class classification by leveraging quantum circuits. To conduct multi-class classification, we utilize QCNN with POVM as well as QNN with PVM. In addition, we propose a probability amplitude regularizer, which fits the probability distribution of observables to the probability distribution of classification. Via extensive results, we corroborate that our proposed PVM-based QML for multi-class classification which outperforms SOTA.

Our future work directions are as follows, *i.e.*, (1) quantum reinforcement learning with the large action spaces or multi-agent setting will be available using less qubits and (2) quantum object detection can be possible by leveraging POVM for bounding box prediction and PVM for classification.



## REFERENCES

- [1] J. Gambetta, “Our new 2022 development roadmap,” *IBM Quantum Computing*, May 2022.
- [2] F. Arute, K. Arya, R. Babbush, D. Bacon, J. C. Bardin, R. Barends, R. Biswas, S. Boixo, F. G. Brandao, D. A. Buell *et al.*, “Quantum supremacy using a programmable superconducting processor,” *Nature*, vol. 574, no. 7779, pp. 505–510, 2019.
- [3] J. Biamonte, P. Wittek, N. Pancotti, P. Rebentrost, N. Wiebe, and S. Lloyd, “Quantum machine learning,” *Nature*, vol. 549, no. 7671, pp. 195–202, 2017.
- [4] Y. Xiong, S. X. Ng, G.-L. Long, and L. Hanzo, “Dual-frequency quantum phase estimation mitigates the spectral leakage of quantum algorithms,” *IEEE Signal Processing Letters*, vol. 29, pp. 1222–1226, 2022.
- [5] S. Du, Y. Yan, and Y. Ma, “Quantum-accelerated fractal image compression: An interdisciplinary approach,” *IEEE Signal Processing Letters*, vol. 22, no. 4, pp. 499–503, 2015.
- [6] J. Park, S. Samarakoon, A. Elgabli, J. Kim, M. Bennis, S.-L. Kim, and M. Debbah, “Communication-efficient and distributed learning over wireless networks: Principles and applications,” *Proceedings of the IEEE*, vol. 109, no. 5, pp. 796–819, May 2021.
- [7] I. Cong, S. Choi, and M. D. Lukin, “Quantum convolutional neural networks,” *Nature Physics*, vol. 15, no. 12, pp. 1273–1278, 2019.
- [8] H. Baek, W. J. Yun, and J. Kim, “Scalable quantum convolutional neural networks,” *CoRR*, vol. abs/2209.12372, 2022.
- [9] I. Nikoloska and O. Simeone, “Training hybrid classical-quantum classifiers via stochastic variational optimization,” *IEEE Signal Processing Letters*, vol. 29, pp. 977–981, 2022.
- [10] W. J. Yun, J. Park, and J. Kim, “Quantum multi-agent meta reinforcement learning,” *CoRR*, vol. abs/2208.11510, 2022.
- [11] W. J. Yun, Y. Kwak, J. P. Kim, H. Cho, S. Jung, J. Park, and J. Kim, “Quantum multi-agent reinforcement learning via variational quantum circuit design,” in *Proc. IEEE International Conference on Distributed Computing Systems (ICDCS)*, Bologna, Italy, July 2022.
- [12] W. J. Yun, J. P. Kim, S. Jung, J. Park, M. Bennis, and J. Kim, “Slimmable quantum federated learning,” in *Proc. ICML Workshop on Dynamic Neural Networks (ICML-DyNN)*, Baltimore, MD, USA, July 2022.
- [13] Y. Kwak, W. J. Yun, S. Jung, and J. Kim, “Quantum neural networks: Concepts, applications, and challenges,” in *Proc. IEEE International Conference on Ubiquitous and Future Networks (ICUFN)*, Jeju Island, S. Korea, August 2021, pp. 413–416.
- [14] M. Cerezo, G. Verdon, H.-Y. Huang, L. Cincio, and P. J. Coles, “Challenges and opportunities in quantum machine learning,” *Nature Computational Science*, vol. 2, no. 9, pp. 567–576, 2022.
- [15] A. Pesah, M. Cerezo, S. Wang, T. Volkoff, A. T. Sornborger, and P. J. Coles, “Absence of barren plateaus in quantum convolutional neural networks,” *Physics Review X*, vol. 11, p. 041011, October 2021.
- [16] S. Y.-C. Chen and S. Yoo, “Federated quantum machine learning,” *Entropy*, vol. 23, no. 4, p. 460, 2021.
- [17] M. Chehimi and W. Saad, “Quantum federated learning with quantum data,” in *Proc. IEEE International Conference on Acoustics, Speech, & Signal Processing (ICASSP)*, Singapore and China, May 2022, pp. 8617–8621.
- [18] T. Hur, L. Kim, and D. K. Park, “Quantum convolutional neural network for classical data classification,” *Quantum Machine Intelligence*, vol. 4, no. 1, pp. 1–18, 2022.
- [19] J. Kim, J. Huh, and D. K. Park, “Classical-to-quantum convolutional neural network transfer learning,” *CoRR*, vol. abs/2208.14708, 2022.
- [20] J. Zheng, Q. Gao, J. Lü, M. Ogorzałek, Y. Pan, and Y. Lü, “Design of a quantum convolutional neural network on quantum circuits,” *Journal of the Franklin Institute*, 2022.
- [21] H. Baek, W. J. Yun, and J. Kim, “3D scalable quantum convolutional neural networks for point cloud data processing in classification applications,” *CoRR*, vol. abs/2210.09728, 2022.
- [22] Y. Chen, “Quantum dilated convolutional neural networks,” *IEEE Access*, vol. 10, pp. 20 240–20 246, 2022.
- [23] S. Choe and M. Perkowski, “Continuous variable quantum mnist classifiers—classical-quantum hybrid quantum neural networks,” *Journal of Quantum Information Science*, vol. 12, no. 2, pp. 37–51, 2022.
- [24] L. Bianchi, J. Pereira, and S. Pirandola, “Generalization in quantum machine learning: A quantum information standpoint,” *PRX Quantum*, vol. 2, no. 4, p. 040321, 2021.
- [25] K. Jacobs, *Quantum measurement theory and its applications*. Cambridge University Press, 2014.
- [26] N. Killoran, T. R. Bromley, J. M. Arrazola, M. Schuld, N. Quesada, and S. Lloyd, “Continuous-variable quantum neural networks,” *Physical Review Research*, vol. 1, no. 3, p. 033063, 2019.
- [27] A. Pérez-Salinas, A. Cervera-Lierta, E. Gil-Fuster, and J. I. Latorre, “Data re-uploading for a universal quantum classifier,” *Quantum*, vol. 4, p. 226, February 2020.
- [28] S. Jerbi, C. Gyurik, S. Marshall, H. J. Briegel, and V. Dunjko, “Variational quantum policies for reinforcement learning,” in *Proc. Conference on Neural Information Processing Systems (NeurIPS)*, Virtual, December 2021.
- [29] P.-Y. Chen, H. Zhang, Y. Sharma, J. Yi, and C.-J. Hsieh, “ZOO: Zeroth order optimization based black-box attacks to deep neural networks without training substitute models,” in *Proc. ACM Workshop on Artificial Intelligence and Security*, November 2017.
- [30] G. E. Crooks, “Gradients of parameterized quantum gates using the parameter-shift rule and gate decomposition,” *CoRR*, vol. abs/1905.13311, 2019.
- [31] T. Sleator and H. Weinfurter, “Realizable universal quantum logic gates,” *Physical Review Letters*, vol. 74, no. 20, p. 4087, 1995.
- [32] H. Wang, Y. Ding, J. Gu, Y. Lin, D. Z. Pan, F. T. Chong, and S. Han, “QuantumNAS: Noise-adaptive search for robust quantum circuits,” in *Proc. IEEE International Symposium on High-Performance Computer Architecture (HPCA)*, Los Alamitos, CA, USA, April 2022, pp. 692–708.